

CCAT-P BOT PUCK TOWER DESIGN

With gratitude to Prof. Dmitry Savransky for his guidance in supervising this project

Kevin Liu (ktl29)

December 18, 2019

1 Abstract

The CCAT-p wall climbing robot is designed to aid in the metrology of the CCAT-p telescope. The goal is to create a robot that can precisely deliver a retro-reflector to specified locations on the telescope mirror, which will allow a laser metrology system to measure the shape and orientation of the mirror. Throughout the semester, the design and analysis of the robot were refined to satisfy the requirements imposed by the telescope and metrology system. This report focuses on the analysis and design of the structure that supports the retro-reflector, and outlines a design that will be able to satisfy requirements. There is also discussion on other progress through the semester, and possible future steps for the development of the project.

Contents

1	Abstract	2
2	Introduction	4
3	Relevant Requirements	4
4	Background	6
5	Semester Timeline	7
6	Puck Tower Redesign	7
6.1	Problem Statement	7
6.2	Analysis	8
6.2.1	Thermal Expansion	9
6.2.2	Thermal Drift of Proximity Sensor	10
6.2.3	Resolution of the Proximity Sensor	12
6.2.4	Unfilterable Vibration Induced by Fans	12
6.2.5	Height error induced by robot tilt	12
6.3	Design	13
6.4	Manufacturing	15
6.5	Assembly	16
7	Testing	16

8 Possible Future Iterations	16
9 Conclusion	18

2 Introduction

The CCAT-p wall climbing robot is being developed to serve the CCAT-prime telescope, a 6 meter diameter telescope currently being developed in the Atacama desert of Chile. The purpose of the robot is to position a retro-reflector (cat's eye or puck) at specified locations on the mirror surface to allow laser metrology measurements to be taken. An example of such a system from Etalon is shown in Figure 1.

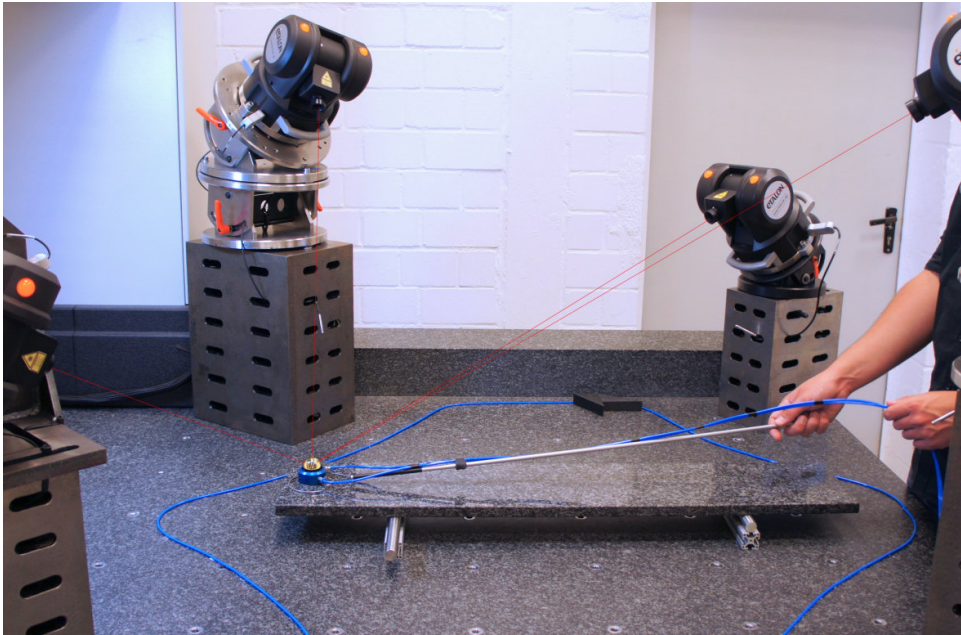


Figure 1: Example of laser metrology system from Etalon [1]

The telescope consists of two mirrors, which themselves consist of 78 and 87 separate aluminum panels. The panels are mounted on actuators which can adjust the orientation and deformation of each panel. A diagram of the telescope is shown Figure 2. In order to calibrate the mirror segments, the orientation and location of the segments must be known. This will be accomplished by measuring five points on each segment using a laser measuring system provided by Etalon. The CCAT-p robot will be required to position the cat's eye to the specified location, while maintaining a level of repeatability both in position on each segment and height from the mirror surface.

3 Relevant Requirements

The CCAT-p robot requirements were derived from requirements from the telescope board and Etalon. The requirements that are relevant to this report are listed below.

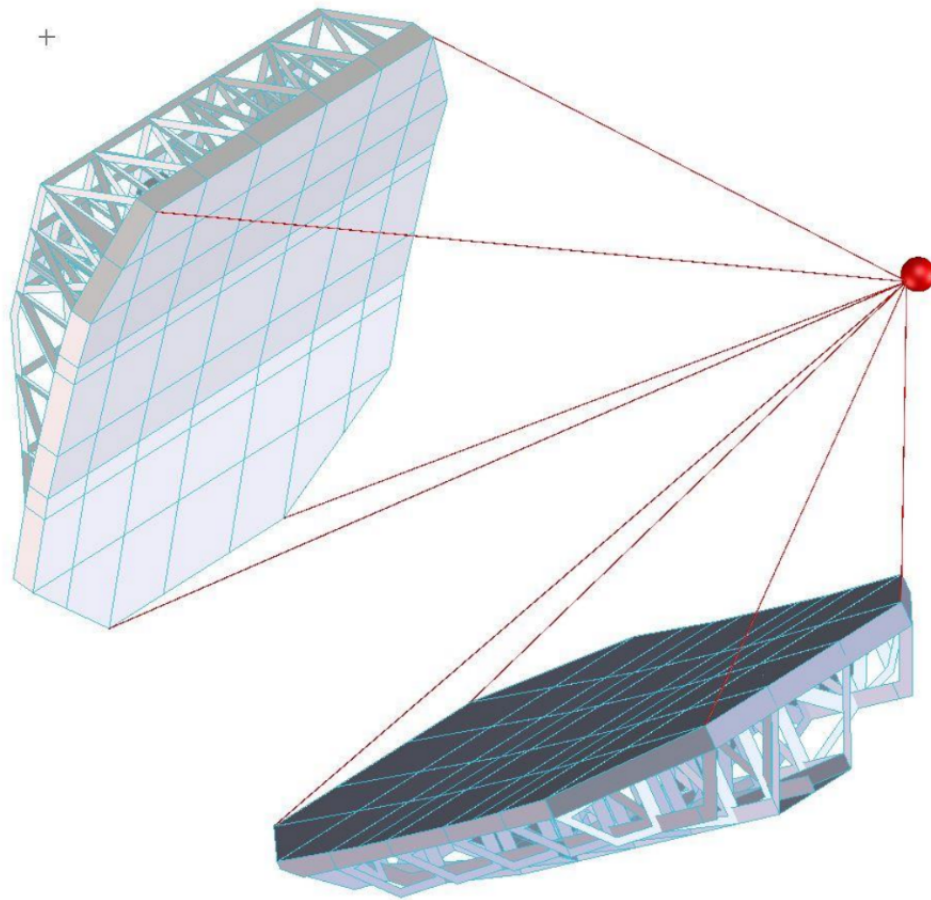


Figure 2: Diagram of planned CCAT-p telescope

1. The suction force of the fan shall exceed the weight of the robot under 50 kPa air pressure conditions.
2. The robot shall be able to operate from -21° C to $+9^{\circ}$ C
3. The robot shall be able to determine the puck's position on a panel to 1 cm accuracy.
4. The puck shall be unobscured for a 120 degree field of view (FOV) with a 10 mm beam width.
5. The measurement of the puck's distance from the mirror surface shall be repeatable to within 1 micron RMS.

4 Background

At the start of the fall 2019 semester, the team had developed an initial prototype and was in the process of developing a second prototype. The first prototype was an adaptation of a commercial robot, which demonstrated the feasibility of a wall climbing robot and the project as a whole. An exploded view of the second prototype is shown in Figure

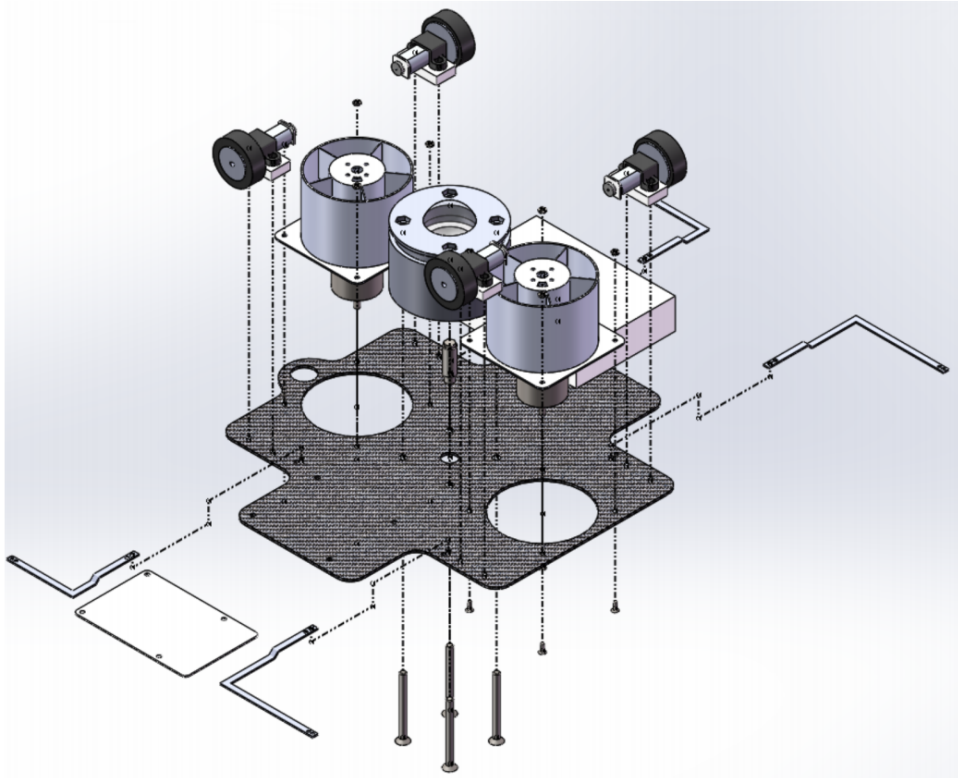


Figure 3: Exploded view of second prototype CAD

3. The second prototype consisted of a four wheel drive robot with two fans for suction. The puck was mounted on a puck tower between the fans. In addition, an Eddy current sensor was placed inside the puck tower to measure the displacement between the mirror surface and the robot chassis. This was in order to satisfy the repeatability requirement of the puck distance from the mirror surface. The suction force of the fans, vibrations, thermal expansion, and more could cause the distance between the mirror surface and the puck to vary, causing a metrology measurement of the puck to be an inaccurate measurement of the mirror surface. A precise proximity sensor such as an Eddy current sensor mounted on the robot that deflects with the robot limits this variability and allows the repeatability requirement to close.

At the onset of the semester, the second prototype's design was mostly complete, but it had yet to demonstrate wall-climbing capabilities. The fans that were being used at the time were not powerful enough. In addition, the team previously believed the cat's eye only needed to be unobstructed for 120° FOV. However, Etalon clarified that the FOV required was 120° with a 10 mm beam width, effectively increasing the required unobstructed volume. Also the size of the cat's eye changed from 40 mm diameter to 30 mm diameter. This required a redesign of the puck tower to mount the cat's eye without any obstruction of the laser system. Finally, after additional analysis it was found that the Eddy current sensor system would not be able to satisfy the height repeatability requirement when thermal drift effects were accounted for, so a solution to this issue was sought after.

5 Semester Timeline

The most immediate deadline this semester was the December Etalon test, where members of the team would bring the robot to Etalon's testing facility in Germany to test the metrology system with the robot. The goals of the tests were to characterize the vibrations induced by the fans, demonstrate that the robot could hold on a vertical wall without slipping, and generally demonstrate that the robot could operate with the metrology system.

From a longer term perspective, the issues previously mentioned with the Eddy current sensor repeatability, as well as long lead times on components necessitated a subsequent iteration of the robot that would need to be developed in the spring of 2020 and beyond.

As a result, two parallel paths were worked on: One which would quickly bring the prototype up to accomplish the December testing goals, and one that would fulfill the project requirements long term.

6 Puck Tower Redesign

6.1 Problem Statement

The puck tower must secure the puck, allow 120° FOV with a 10 mm beam width, and maintain the measurement of the distance between the center of the puck and mirror surface to be repeatable within 1 micron. The puck is a 30 mm diameter sphere made of PSF68 glass. When the 120° FOV with a 10 mm beam width is imposed on the puck,

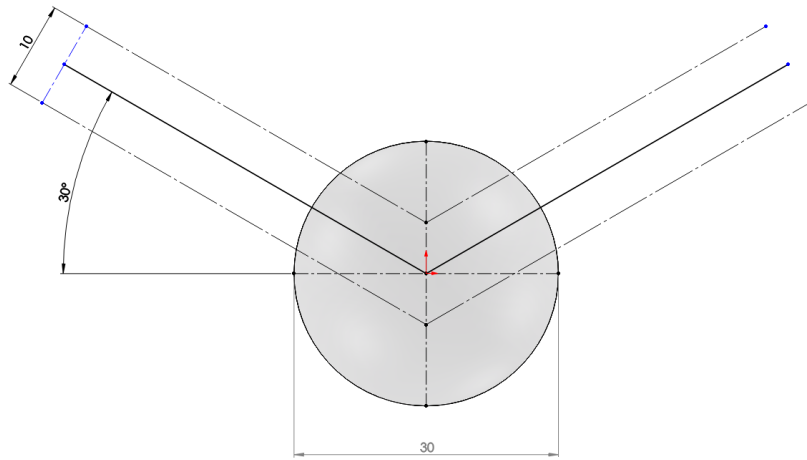


Figure 4: Cat's eye FOV geometry

it can be shown geometrically that approximately the top half of the sphere must be unobstructed. Figure 4 shows the geometry of the laser beam and why the unobstructed region is larger than only the top 120° . Because the top 180° FOV must be unobstructed, no mounting can obstruct the top half of the cat's eye. As a result, an adhesive must be used to secure the puck from the bottom half, permanently bonding the tower to the puck. It should be noted, however, that the exact FOV requirements still appear to be liable to change, and more severe or lenient requirements could be determined in the future.

In addition, the puck tower must house and mount a proximity sensor to measure the displacement of the puck from the mirror surface. The sensor should be concentric with the puck to have the most accurate correlation between sensor measurement and puck displacement.

6.2 Analysis

The error budget of the displacement is 1 micron. There are multiple sources of error that combine to detract from our error margin. These include

- Thermal expansion of the puck tower
- Thermal drift of the proximity sensor
- Resolution of the proximity sensor
- Unfilterable vibration induced by the fans

- Height error induced by robot tilt

6.2.1 Thermal Expansion

The proximity sensor provides a measure of distance of the robot from the mirror surface. However, there is a distance between the center of the puck to the measuring end of the proximity probe. As a result, thermal fluctuations will cause a change in the height of the puck that is not measured by the sensor, and these fluctuations decrease the error margin.

The robot operates in a 30° C range. However, each calibration is planned to be completed within 1 hour, and based on the operating environment of the telescope, we assume that the temperature will not fluctuate more than 10° C over the course of an hour.

A diagram of the puck tower is shown in Figure 5. The probe is mounted using hex nuts to a plate with thickness A . Then the puck tower is mounted to the sensor plate and has length B . Finally the distance between the center of the puck and where the puck contacts the puck tower is length C .

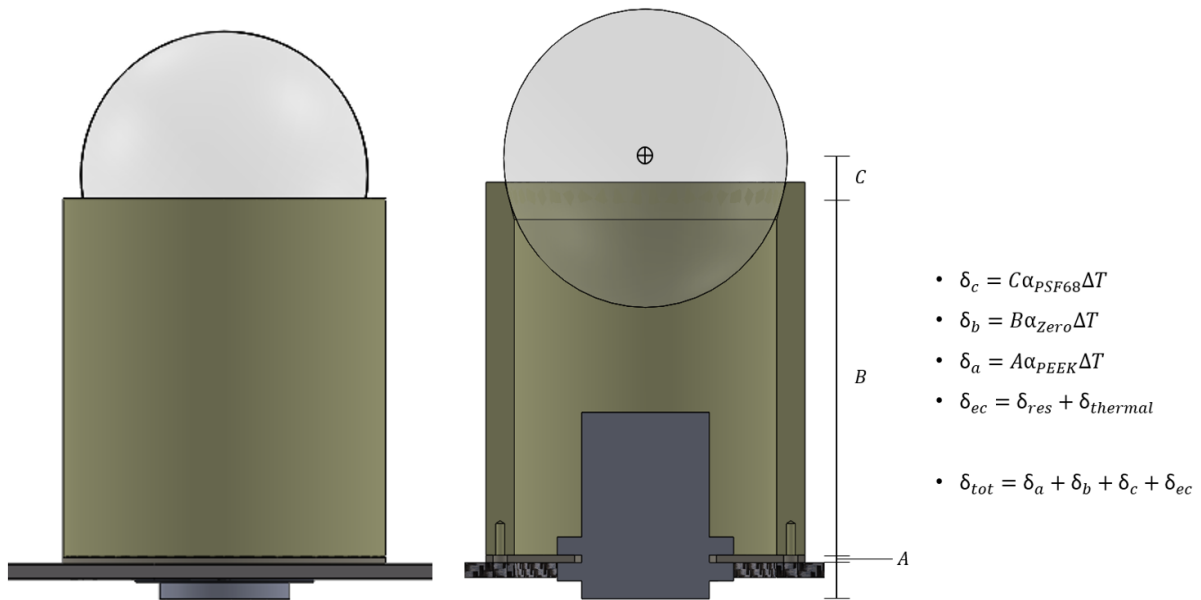


Figure 5: Thermal expansion diagram

The total displacement change is the sum of the expansion of each component. Each displacement depends on the length, the coefficient of thermal expansion of the material,

and the magnitude of temperature change.

$$\delta = l\alpha\Delta T \quad (1)$$

The FOV requirement drives the puck to a minimum height, which is determined by the height and position of the fans. The top of the fans must not obscure the puck's FOV. From this, a baseline design assigns the dimensions as $A = 1$ mm, $B = 50$ mm, $C = 1$ mm.

The dimension B is much larger than the other dimensions, so if the thermal expansion coefficient of each material were similar, the expansion due to B would dominate the thermal expansion. Assuming the temperature increases 10° C and using aluminum, which has a thermal expansion coefficient of $22 \frac{\text{mm}}{\text{mm K}}$ [2], the puck tower expands 11 microns. Clearly, this greatly exceeds our error budget, meaning that the puck tower must be made with a material that has a much lower CTE.

A candidate material is ZERODUR, a low thermal expansion glass from SCHOTT with $\alpha = 0 \pm 0.1 \times 10^{-6} \text{ K}^{-1}$ [3].

Using ZERODUR for the puck tower and PEEK for the sensor plate, we find that the thermal expansion is 0.14 microns.

$$\begin{aligned} \delta_{\text{therm}} &= \delta_a + \delta_b + \delta_c \\ &= A\alpha_{\text{PEEK}}\Delta T + B\alpha_{\text{ZERODUR}}\Delta T + C\alpha_{\text{PSF68}}\Delta T \\ &= (1 \times 10^{-3}) \cdot 0.9 \cdot 10 + (50 \times 10^{-3}) \cdot 0.1 \cdot 10 + (1 \times 10^{-3}) \cdot 8.4 \cdot 10 \\ &= 0.01 + 0.05 + 0.08 \\ &= 0.14 \text{ microns} \end{aligned}$$

6.2.2 Thermal Drift of Proximity Sensor

The proximity sensor selected previous to this semester was the Lion Precision ECL101-U8 Eddy current sensor. The amount of thermal drift is

$$\delta_{\text{tdrift}} = r \cdot s \cdot \Delta T \quad (2)$$

where r is the sensor range and s is the probe thermal drift.

According to the specifications of the sensor, the sensor range is 2 mm, the probe thermal drift at mid-range is $0.04\%(\text{°C})^{-1}$ [4]. As a result the predicted thermal drift is

8 microns.

$$\begin{aligned}\delta_{\text{tdrift}} &= 2 \times 10^3 \cdot 0.04 \times 10^{-2} \cdot 10 \\ &= 8 \text{ microns}\end{aligned}$$

This calculation shows that with the required temperature range, the Eddy current sensor will not be able to satisfy the 1 micron repeatability requirement.

There are a couple options to help resolve this issue. Additional analysis and testing could narrow the temperature range to decrease the required temperature delta. The sensor range could also be reduced so that even with the same thermal drift percentage, the absolute thermal drift magnitude would decrease. However, there is a minimum limit to how far the range can be reduced, because there would be a large risk of the probe contacting the mirror surface and damaging the probe.

Another possible solution is to add a temperature feedback system to maintain a constant temperature to the robot. Alternatively a temperature sensor could be used to post-process the data and subtract the predicted thermal expansion.

The most promising solution is to replace the Eddy current sensor with a capacitive sensor, a probe that measures the capacitance between conducting surfaces. These sensors have much lower thermal drifts. The downside of capacitive sensors is that they need to operate in a clean environment. In particular, a film of oil or water on the mirror surface would greatly influence the capacitance measured and result in an inaccurate measurement. Fortunately, there should be no such contamination at the telescope site. At most there will be a small amount of dust which will have a negligible effect on the sensor.

A candidate sensor is the Micro-Epsilon capaNC DT6110-CS05M8. According to its specifications, it has a probe thermal drift of $-10 \frac{\text{mm}}{\text{K}}$ [5] and a controller temperature stability of 200 ppm. The controller stability is based on the full scale output (FSO), which for the probe is 4.1 mm. This results in a thermal drift of 0.1 microns.

$$\begin{aligned}\delta_{\text{tdrift}} &= 0.01 \cdot 10 + 200 \times 10^{-6} * 4.1 \times 10^3 \\ &= 0.1 \text{ microns}\end{aligned}$$

Therefore the Micro-Epsilon capacitive sensor could allow the repeatability requirement to close for the future iteration of the robot.

6.2.3 Resolution of the Proximity Sensor

The repeatability of the measurement depends on the resolution of the proximity sensor. The Lion Eddy current sensor has a resolution of 0.1 microns at 1 kHz.

The resolution of the Micro-Epsilon sensor is a combination of the controller and probe resolution. The controller resolution is 0.015% FSO at 1 kHz. The probe has a resolution of approximately 10 nm. This results in a δ_{res} of 0.63 microns.

6.2.4 Unfilterable Vibration Induced by Fans

The fans of the robot induce vibrations in the robot and the mirror panel. The positions on the mirror are selected above the actuator positions, resulting in higher stiffness and less vibration. Nonetheless, some vibration will be induced. The measurement of importance is the average height of the puck over the measurement period. Therefore we will need to demonstrate that the vibrations induced are repeatable to within the error budget through testing. Analysis from the Etalon test will better characterize this level of vibration.

If the vibration is too large, options include minimizing the mass of the robot, allowing less power to be inputted to secure the robot to the mirror.

6.2.5 Height error induced by robot tilt

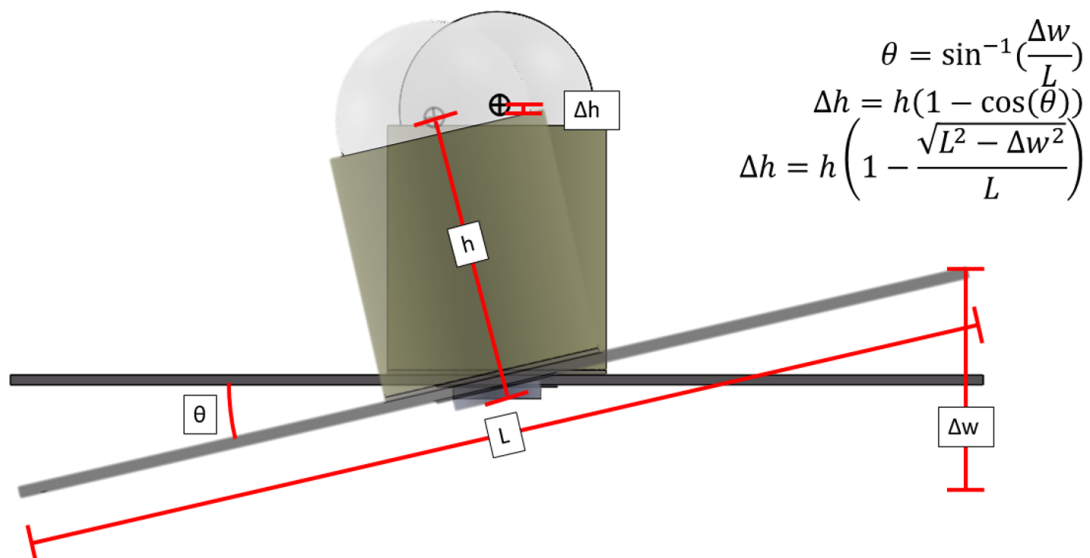


Figure 6: Tilt error diagram

If the suction force of the fans is not symmetric on the robot, the robot could tilt. If the puck tower is not normal to the mirror surface, the center of the puck will be closer to the mirror surface than expected. The change in height is

$$\Delta h = h \left(1 - \frac{\sqrt{L^2 - \Delta w^2}}{L} \right) \quad (3)$$

where h is the height of the puck, L is the wheel base, and Δw is the change in difference in height between the wheels. Assuming $h = 50$ mm, $L = 100$ mm, a Δw of 0.6 mm results in 1 micron of Δh .

Testing will need to be conducted verify that the tilt is sufficiently low.

6.3 Design

After analyzing the error budget, the design that we will move forward with is a ZERODUR puck tower with a 30 mm cat's eye glued to the puck tower. A Micro-Epsilon capacitive sensor will be mounted to a PEEK sensor plate, which is in turn mounted to the puck tower and robot chassis.

However, for the purposes of the December Etalon test, we chose to continue using the Eddy current sensor and use an aluminum puck tower for reasons involving budget and lead time. The following discussion will cover the design decisions for the puck tower used on the Etalon test.

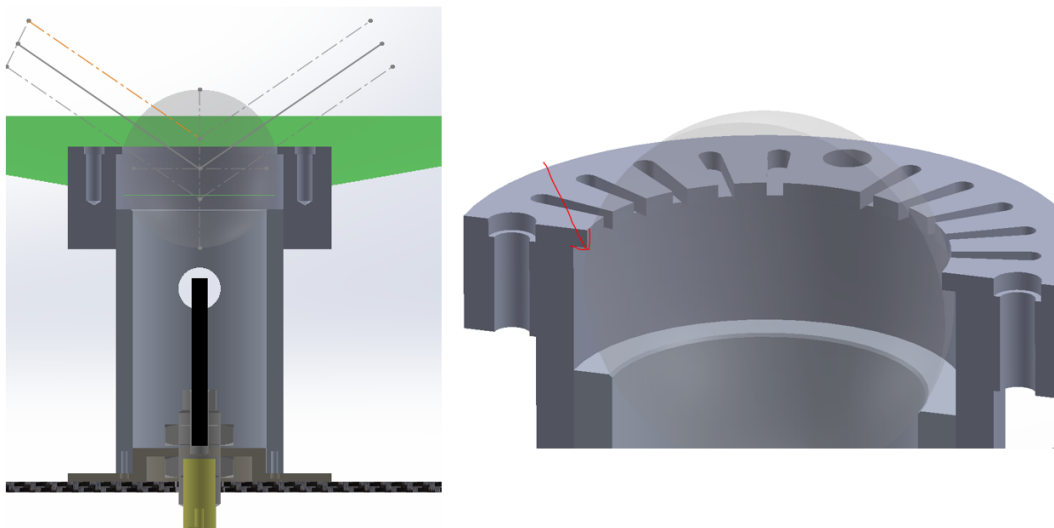


Figure 7: Etalon test puck tower

A cross section of the temporary puck tower made for the Etalon test is shown in

Figure 12.

The decision was made to have a puck tower cap that would secure the cat's eye without requiring permanent adhesion. The presence of the cap limits the FOV to 120° for the Etalon test, which was communicated to Etalon. The cap was designed as a sleeve that slides over the puck tower and has mounting holes for an acrylic disc to compress the puck to the tower. Where the acrylic disk contacts the puck is highlighted with an arrow in Figure 12. The restraining force on the puck is a result of the deflection of the acrylic disk onto the puck. As a result, the shape of the acrylic disk was designed to have a stiffness that would deflect without breaking while providing a restraining force. CAD images of the cap and the acrylic disk are shown in Figures 8 and 9. A CAD of the puck

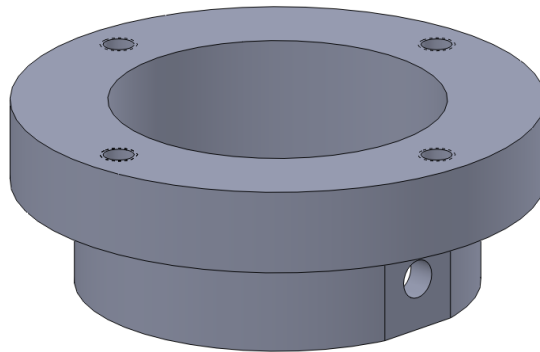


Figure 8: CAD of puck tower cap

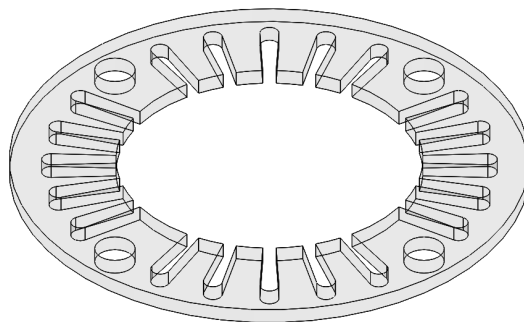


Figure 9: CAD of acrylic disk

tower is shown in Figure 10. The puck tower is hollow and houses the proximity sensor in its interior. The puck tower also has a hole drilled in the side to allow the harness of the Eddy current sensor to pass through. The tower is mounted to the sensor plate using four countersunk M1.6 x 0.35mm screws.

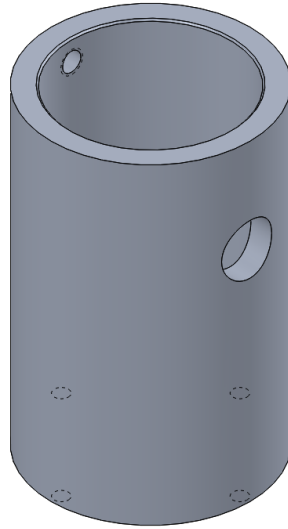


Figure 10: CAD of puck tower

The sensor plate has four through holes to allow the M1.6 x 0.35mm screws to fasten to the puck tower. It also has four M3.5 through holes to allow the sensor plate and puck tower assembly to be fastened to the chassis. A CAD image of the sensor plate is shown in Figure 11.

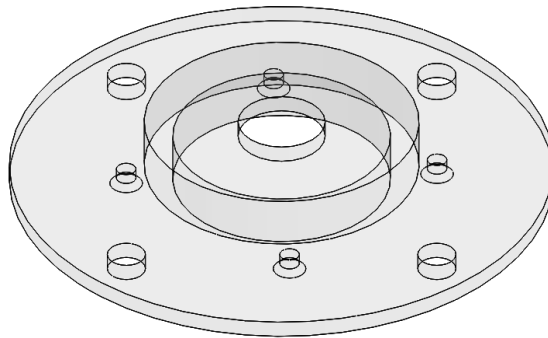


Figure 11: CAD of sensor plate

6.4 Manufacturing

The puck tower and puck tower cap were machined out of Al6061-T6. The puck tower began as a stock tube of aluminum. First, the tube was cut to length on the lathe. A chamfer was applied to the lip of the tube that the cat's eye will contact. Then the tube was brought to the mill, where the four M1.6 threaded holes, harness through hole, and

cap threaded hole were machined. In addition, thin strips of duct tape were applied to the chamfered lip to provide a non-abrasive surface for the cat's eye to contact.

The puck tower cap was first cut to length of the lathe. Then it was brought to the mill to machine holes for the acrylic disk to fasten to and the hole to allow the cap to secure to the puck tower.

The sensor plate and puck cap disk were each laser-cut from 1.5mm thick acrylic. To create the sensor plate, multiple disks were epoxied together to raise the sensor to the correct height. A chamfer was also applied to the M1.6 through holes to allow the sensor plate to lie flush with the chassis.

6.5 Assembly

All of the components were assembled together to form the puck tower, and the puck tower was then installed to the robot. A picture of the robot is shown in Figure 12. There were no issues assembling, but it was noted that installing the puck tower to the robot was difficult because the wiring on the robot was difficult to clear.

7 Testing

The assembly and operation of the puck tower was communicated to the members of the team that would travel to Germany. In December, the team successfully brought the robot to Etalon and the puck tower performed as expected. The puck was installed onto the tower and testing was conducted successfully.

8 Possible Future Iterations

Through the course of the semester the team saw possible improvements that could be implemented for future iterations of the robot, which I will discuss in this section.

- Adjustable height of probe - The current design for the sensor plate makes adjusting the height of the probe to be cumbersome. The tower must be disassembled, and the hex nuts securing the probe must be adjusted. In future designs there is a desire for an easier method to adjust the height of the probe.
- Two wheel drive - The current design has four independent wheels driving using differential drive. However, a true differential drive only has two controlled wheels

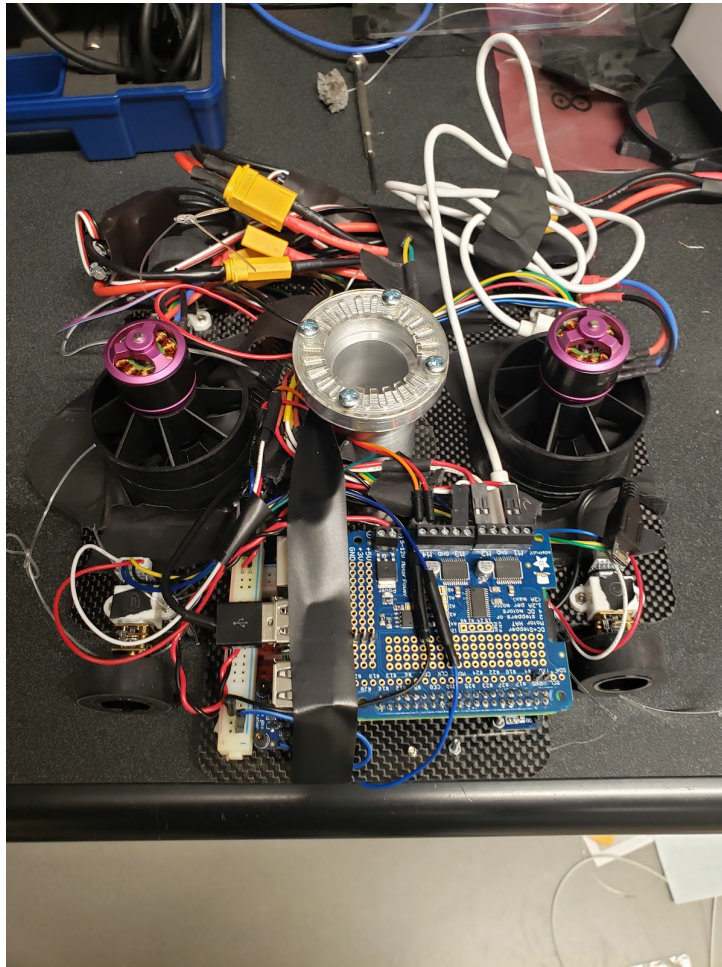


Figure 12: Etalon test puck tower

and additional caster wheels. The reason four wheels is an issue is that the instantaneous center of rotation of a differential drive must be in line with the two controlled wheels. Therefore, with four wheels the robot is unable to turn without wheels slipping on the ground. As a result, it may be difficult to have repeatable and precise turning. A possible solution is to use two controlled wheels and use additional caster wheels.

- Use one fan - The current design has two fans that are positioned near the edge of the robot chassis. However, this does not appear to be the most efficient use of the fans, as the low pressure flow does not act on much of the robot chassis. A more efficient fan could be one large fan in the center of the chassis so that there is an even spread of low pressure. The downside to this solution is that the robot is no longer symmetric, which could have negative consequences with the tilt and

vibration of the robot.

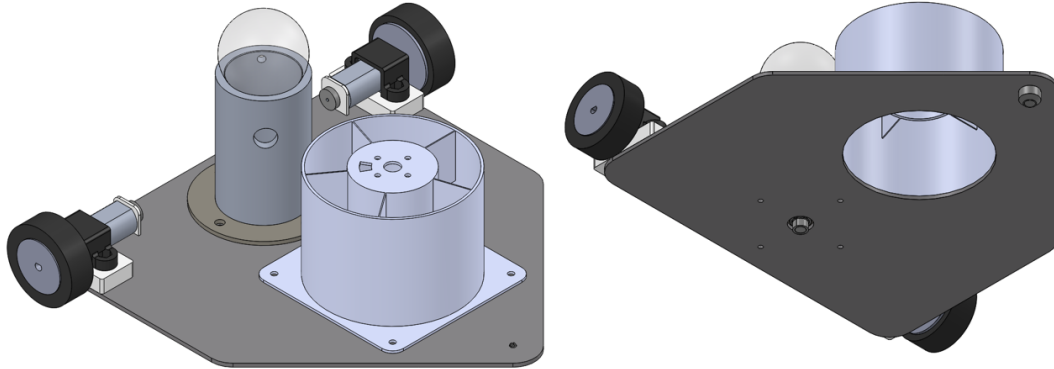


Figure 13: Possible design iteration minimizing mass

Figure 13 shows a concept of a future robot iteration. The use of the single fan greatly decreases the mass of the robot and the power requirements of the robot. Also, only using two controlled wheels decreases the mass and complexity of the controls system. However the loss of symmetry could be a downside that would be identified through testing.

9 Conclusion

Over the course of the semester significant progress occurred on the project, and the team successfully sent a working robot to Etalon in Germany for system tests. At the start of the semester, the robot was incapable of climbing walls and the the puck tower needed to be redesigned. By the end of the semester the robot was able to climb walls and integrate with the cat's eye. Future work remains to ensure the robot will be able to climb walls safely at low pressures. In addition more work needs to be done to satisfy the repeatability requirement.

References

- [1] "Animation Kalibrierung Von Linearachsen / Calibration of Linear Axes." Etalon GmbH Part of Hexagon LaserTRACERNG, www.etalon-gmbh.com/en/products/lasertracer/.
- [2] "Coefficients of Linear Thermal Expansion." Engineering ToolBox, www.engineeringtoolbox.com/linear-expansion-coefficients-d_95.html.

- [3] “ZERODUR® Extremely Low Expansion Glass Ceramic.” SCHOTT,
www.us.schott.com/advanced_optics/english/products/optical-materials/zerodur-extremely-low-expansion-glass-ceramic/zerodur/index.html.

- [4] “Eddy-Current Sensors.” Lion Precision,
www.lionprecision.com/products/eddy-current-sensors/.

- [5] “Capacitive Displacement Sensors and Measurement Systems.” Micro-Epsilon, 2019,
www.micro-epsilon.com/displacement-position-sensors/capacitive-sensor/.